Available online at www.sciencedirect.com
SCIENCE DIRECT®
Journal of Crystal Growth 275 (2005) 474–480
JOURNAL OF CRYSTAL GROWTH
www.elsevier.com/locate/jcrysgro

Influence of Sb and Y co-doping on properties of $PbWO_4$ crystal

Jianjun Xie[a,*], Peizhi Yang[a], Hui Yuan[a], Jingying Liao[a], Bingfu Shen[a], Zhiwen Yin[a], Dunhua Cao[b], Mu Gu[b]

[a]*Shanghai Institute of Ceramics, Chinese Academy of Sciences, Crystal Centre, 1295 Dingxi Road, Shanghai 200050, China*
[b]*Department of Physics, Tongji University, Shanghai 200092, China*

Received 9 September 2004; accepted 9 December 2004
Communicated by M. Schieber
Available online 19 January 2005

Abstract

This paper presents the growth of co-doped $PbWO_4$:(Sb,Y) crystal by modified Bridgman method and the influence of Sb and Y co-doping on luminescence and scintillation properties of $PbWO_4$ crystal. Based on the results of measuring the optical transmission, X-ray excited luminescence, photoluminescence, thermoluminescence, light yield and decay time of $PbWO_4$:(Sb,Y) crystal, it can been seen that at the concentration involved in the study the $PbWO_4$:(Sb,Y) crystal has higher light yield and sharper optical absorption edge. The maximum light yield of 55 p.e./MeV was obtained in co-doped $PbWO_4$:(Sb,Y) crystal with bialkali photomultiplier for a fixed condition of the crystal size of $23 \times 23 \times 20\,mm^3$ and the gate width of 200 ns. However, compared to pure $PbWO_4$ crystal the co-doping of Sb and Y results in a relatively slower decay component.

PACS: 81.10.Fq; 78.20.Ci

Keywords: A1. Doping; A2. Bridgman technique; A2. Single-crystal growth; B1. Lead tungstate; B2. Light yield

1. Introduction

Lead tungstate crystal (PWO) was been reported in the 1940s [1]; however, renewed intensive studies for $PbWO_4$ crystal arose a few years ago, especially after 1994, when it was selected as the most appropriate scintillator in the construction of electromagnetic calorimeter in the compact muon solenoid detector at large hadron collider at CERN [2] because of its many advantages such as the short attention length of 2 cm for gamma rays of 511 KeV, as compared to 3 cm for BGO,

*Corresponding author. Tel.: +86 021 52411011; fax: +86 021 52413122.
E-mail address: jjxie@mail.sic.ac.cn (J. Xie).

0022-0248/$ - see front matter © 2004 Elsevier B.V. All rights reserved.
doi:10.1016/j.jcrysgro.2004.12.028

3.6 cm for LSO, high density (~8.3 g/cm^3), fast decay time with no afterglow, non-hygroscopy and low cost [3,4]. The usage of PWO crystal, however, is limited in high-energy physics community by its low light output. Due to the well-developed technology, relatively low production cost and other advantages of this material, it is worth searching for some ways to increase the light output of lead tungstate, which, would make it suitable for other application communities such as nuclear medical image facilities-positron emission tomograph (PET) scanners. According to specialists of PET scanners, PWO crystal could be successfully used in PET if its light output is increased to ~10% of the BGO scintillator, keeping its present fast rise time for the main component, but tolerating the decay time of a few hundred nanoseconds for the minor component and some expense of the radiation hardness [5]. In recent years Kobayashi et al. [5-8] have widely investigated the effects of doping PWO with different ions on the light yield and other scintillation properties, including single dopant, co-doping, and three dopants. It has been found that Mo^{6+} or F^- ion doping could increase light output of the PWO crystal to about 10% of the BGO crystal [6,8], but it simultaneously produces a red shift of the position of maximum X-ray luminescence and very slow components of decay. Wang et al. Wang et al. [9,10] reported that doping Sb_2O_3 could improve light output and reduce slow decay components even though it was inadequate in improving crystal radiation hardness.

In the present paper, we report the growth and correlated measurements of X-ray excited luminescence (XEL), photoluminescence (PL), thermoluminescence (TL) and decay time of pure PWO and co-doped PWO:(Sb,Y) crystals grown by modified Bridgman method at the concentration of Sb_2O_3: 1000, Y_2O_3: 100 at. ppm, respectively. The effect of Sb and Y co-doping on the properties of PWO crystal is studied carefully. Compared to pure PWO crystal, co-doped PWO:(Sb,Y) crystal at the above doping concentration shows a considerable increase in light output and relatively slower decay kinetics.

2. Experiment methods

Pure PWO and co-doped PWO:(Sb,Y) single crystals were grown by modified Bridgman method in equivalent conditions. The raw materials, 5 N pure PbO and 4 N WO_3 powders were first dried at 200 °C for a day to remove water, then prepared in the precise stoichiometric ratio of PWO in an agate mortar. The charge mixture is first melted at about 25 °C above the melting point of pure PWO in a platinum crucible to ensure complete homogeneity. After heating to high temperature the above melt is poured into a designed thin platinum crucible to form polycrystalline PWO grogs for multi-times crystallization growth. Sb and Y dopants were introduced into the charge mixture in the form of Sb_2O_3 and Y_2O_3 by the initial concentration of ~1000 and ~100 at. ppm, respectively, added in the last crystallization. In order to prevent contamination from out atmosphere and suppress component deviation from stoichiometric composition due to evaporation in air atmosphere, the designed thin platinum crucible was almost sealed completely. Pure and co-doped single crystals were grown along [0 0 1] direction in the experiment. Colorless and crack-free crystal ingots with a size of $25 \times 25 \times 250\,mm^3$ were obtained. No inclusion was found in the pure and doped single crystals except the top ends at about a few centimeters range. The details of schematic of the furnace and crystal growth technology can be seen in Ref. [11]. Samples for optical transmission, XEL and PL measurements were cut into polished plates $10 \times 10 \times 2\,mm^3$ in dimensions, while $23 \times 23 \times 20\,mm^3$ samples with all-polished faces were used for light output and decay kinetics measurements. All samples were cut at the same close-to-seed positions from the parent bulk crystals with their large faces normal to the crystal *c*-axis direction. Samples in XRD experiments were crushed and ball-milled from the above polished plate samples.

The crystal structure was confirmed by powder X-ray diffraction method (Rigaku D/max 2550 V diffracter, Cu Kα). Optical transmission spectra were recorded along the *c*-axis direction of samples by a SHIMAZU-2501PC spectrometer at room

temperature. The XEL spectra were measured on an X-ray excited spectrometer, FluorMain, where a F-30 movable clinical X-ray tube (W anticathode target) was used as the X-ray source, and operated under the same condition (80 kV, 4 mA) at room temperature. The XEL spectra of the samples were obtained by 44 W plate grating monochromator and Hamamatsu R928-28 PMT with the data acquired by computer. PL spectra were taken with a fluorescence spectrometer, a Perkin-Elmer LS-55, which has a Xe lamp as an excitation source. Decay kinetics measurements were performed under pulsed X-ray and detected by photomutiplier XP2020Q at 295 K. Light output at 20 °C was measured by using a ^{137}Cs γ-ray source and Philip XP2262B PMT on QVT Multichannel Analyzer test bench with a gate width of 200 ns. The TL glow curves measurement after UV light irradiation was made at room temperature by FJ-427A TL spectrometer with a heating rate of 2 °C/s. A 1000 W high mercury lamp was used as UV light irradiation source to irradiate the samples for 20 min. To compare the radiation damage in pure PWO and PWO:(Sb,Y) block samples, we calculated the light output loss and induced absorption coefficient (μ_{irra}) after carrying out the irradiation experiment with ^{60}Co source at a dose rate of 3500 rad /h for 24 h. μ_{irra} defined as

$$\mu_{irra} = (1/d)\ln(T_0/T), \quad (1)$$

where d is the thickness across which the transmittance T_0 (before irradiation) and T (after irradiation) were measured.

3. Results and discussion

Since the dopants concentration is high, it is necessary to first confirm the structure of as-grown crystals. The phase analysis and lattice parameters measurement of pure PWO and PWO:(Sb,Y) crystals were performed by X-ray diffraction (XRD), Si was used as standard sample. The XRD profiles are shown in Fig. 1. All the peaks were well indexed by tetragonal $I41/a$ in JCPDS cards. The lattice parameters were calculated as follows: $a = b = 0.5464$ nm, $c = 1.2045$ nm and the unit cell volume was 0.35961 nm^3. The inset in the upper section of Fig. 1 is the rocking curve from [0 0 1] oriented polished slice of the as-grown PWO:(Sb,Y) crystal. It can be seen that the diffraction peak appears at $\theta = 14.815°$ in accordance with Fig. 1 ($2\theta = 29.637°$). These results are in agreement with that reported in JCPDS 080476

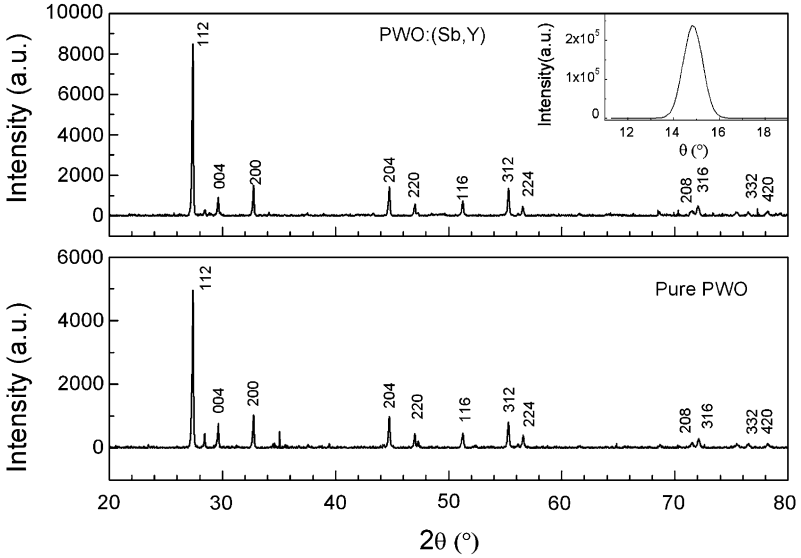

Fig. 1. XRD pattern of pure PWO and PWO:(Sb,Y) crystals grown by modified Bridgman method. Inset in the upper figure: X-ray rocking curve of as-grown PWO:(Sb,Y) crystal.

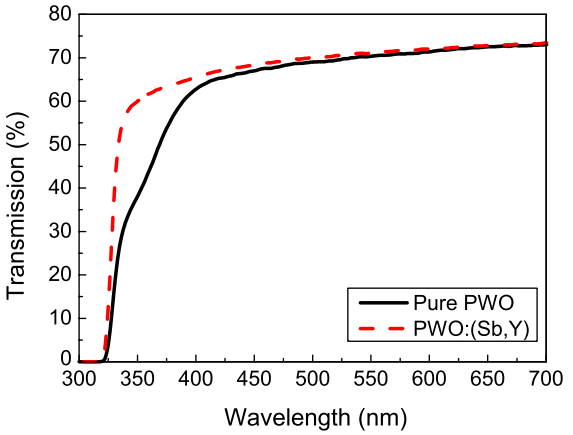

Fig. 2. Optical transmission spectra of pure PWO and PWO:(Sb,Y) crystals.

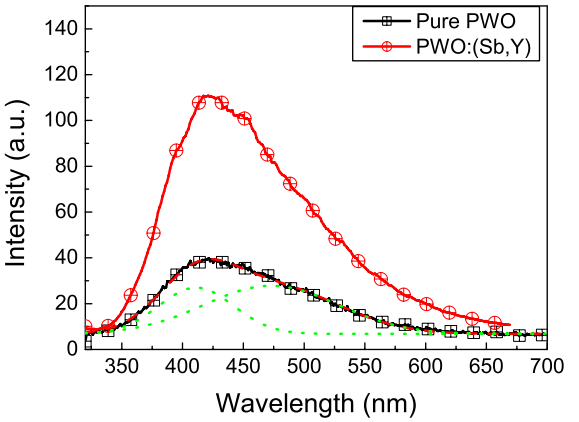

Fig. 3. XEL spectra of pure PWO (square line) and PWO:(Sb,Y) (circle line) crystals. The XEL spectrum of pure PWO crystal is given approximated by two Gaussian fits with separate components given as peaking at about 412 and 480 nm (dot line).

cards and reveal that co-doping of Sb and Y at the designed concentration does not change the crystal structure or induce a new phase. The crystals are homogeneous scheelite structure with good quality and the Sb and Y ions would go into PWO crystal lattice well.

The optical transmission spectra of pure PWO and PWO:(Sb,Y) are shown in Fig. 2. Compared to that of pure PWO, optical transmission in the present PWO:(Sb,Y) single crystal has been improved evidently in the short wavelength 350–420 nm region, and its optical absorption edge is sharper than that of pure PWO.

XEL spectra (Fig. 3) for pure PWO can be defined as a superposition of two Gaussian components with approximate peaking wavelength: $I_1 = 412$ nm, $I_2 = 480$ nm, which are assigned to self-trapped excited blue and blue-green luminescence, respectively. In PWO:(Sb,Y) crystal, additions of Sb and Y ions make the intensity of blue and green luminescence larger. XEL in PWO:(Sb,Y) similar in shape to that of single doped PWO:Sb crystal [9], which showed enhanced blue bands and a blue–green luminescence.

In pure PWO, the excitation spectra of 420 nm-emission (under part in Fig. 4) show a narrow band peaking at 315 nm, a weak broad band at 260 nm, and its main emission ($\lambda_{ex} = 315$ and 260 nm) is a broad band (350–550 nm) peaked at 420 nm. Similar to the XEL spectra, the PL

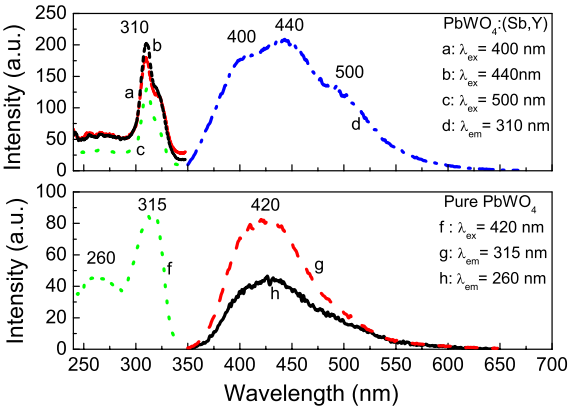

Fig. 4. Upper figure is excitation spectra ((a) $\lambda_{em} = 400$ nm, (b) $\lambda_{em} = 440$ nm, (c)$\lambda_{em} = 500$ nm) and emission spectra ((d) $\lambda_{ex} = 310$ nm, of PWO:(Sb,Y) crystal. The underside is excitation spectra (f) ($\lambda_{em} = 420$ nm, and emission spectra (g) $\lambda_{ex} = 315$ nm, (f) $\lambda_{ex} = 260$ nm) of pure PWO crystal.

intensity of PWO:(Sb,Y) in Fig. 4 was wholly enhanced. Emission spectra of PWO:(Sb,Y) crystal consists of three blue and blue–green bands peaked at about 400, 440 and 490 nm. The main excitation peak slightly shifts to a short wavelength in comparison with that of the pure PWO sample, but the strongest emission peak shifts to a

long wavelength in PWO:(Sb,Y) crystal. It indicates that the co-doping of Sb and Y may have some effect on the energy level of PWO.

The decay curves under pulsed X-ray measurement are shown in Fig. 5 in 200 ns gate width. The mean decay time was calculated using the following two-exponential approximation of decay curve

$$S(t) = \sum_{i=1}^{N} \frac{1}{2} I_i \tau_i^{-1} \exp\left[-\tau_i^{-1}(t - T_0 - \frac{1}{4}\tau_i^{-1}\sigma^2)\right] \left\{\left[1 - \mathrm{erf}\left[\frac{1}{2}\tau_i^{-1}\sigma - (t - T_0)/\sigma\right]\right]\right\}, \quad (2)$$

where N is the fitted number of multi-exponential approximation of the decay curve, τ_I is the mean time and I_i is the relative intensity. The decay kinetics results are listed in Table 1. The decay curve of pure PWO and PWO:(Sb,Y) crystals is approximated by the sum of two exponentials with decay times $\tau_1 = 3.8$ ns and $\tau_2 = 15.9$ ns, and $\tau_1 = 11.0$ and $\tau_2 = 57.1$ ns, respectively. The decay in PWO:(Sb,Y) crystal shows a significant increase in the first component; however, the second decay component becomes slower. From the above experimental results, it can be seen that Sb and Y co-doping in PWO can enhance the intensity of luminescence but give some contributions to the "slow" decay components.

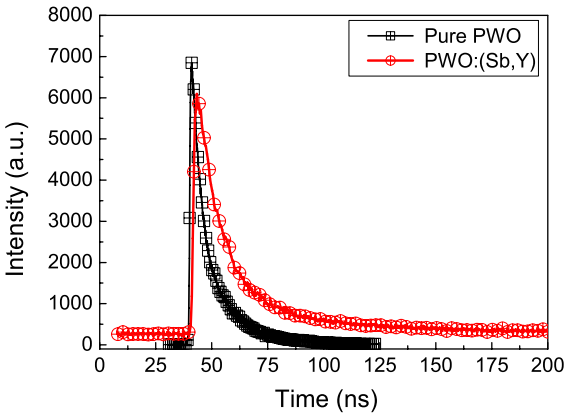

Fig. 5. Luminescence decay kinetics of pure PWO and PWO:(Sb,Y) single crystals under pulsed X-ray excitation at 295 K.

Table 1
The parameters of decay time of pure PWO and PWO:(Sb,Y) crystals in Fig. 5

Sample	τ_1 (ns)	τ_2 (ns)	I_1 (%)	I_2 (%)
Pure PWO	3.8	15.9	33.5	66.5
PWO:(Sb,Y)	11.0	57.1	60.1	39.9

The light output and loss of the pure PWO and PWO:(Sb,Y) within 200 ns gate width is compared in Table 2. Typical increase in LY was obtained for Sb and Y co-doping. Compared to single doping in PWO with Mo, Gd, Sb or Y et al. ions [5,7], the present PWO:(Sb,Y) crystal has a larger light output within 200 ns.

TL glow curves of pure PWO and PWO:(Sb,Y) after UV irradiation for 20 min. were measured at room temperature (Fig. 6). There exist at least two TL peaks between RT and 250 °C in the as-grown pure $PbWO_4$, peaking at around 75 and 155 °C. The 75 °C TL peak might be related to the red emission centers in PWO [12], which was found to be absent in the other stable single charge state trivalent-ion doped samples, leading to low intensity and structureless TL glow curves spectra [7,13]. These peaks almost disappear also for the present PWO:(Sb,Y) crystal studied here, which is a significant lowering sign of intrinsic lattice defects. Although significant suppression of around 75 and 155 °C TL peaks observed in the present PWO:(Sb,Y) suggests similar charge compensation to that in typical stable single charge state trivalent-ion doped PWO, there is another evident difference in the 50–250 °C region between pure $PbWO_4$ and $PbWO_4$:(Sb,Y) crystals. A large broad TL peak in the present PWO:(Sb,Y) crystal appeared with a peak of about 120 °C, indicating that a new electron or hole center was generated due to Sb and Y co- doping. The large broad TL peak in the temperature range 50–200 °C may indicate a possibility of slightly poor radiation hardness of PWO:(Sb,Y) [14]. By comparison to the light output loss (Table 2) and μ_{irra} (Fig. 6 inset) at the same irradiation conditions, it can be seen that the radiation damage of PWO:(Sb,Y) is also larger, close to the pure PWO.

Table 2
The light output and light output loss of pure PWO and PWO:(Sb,Y) crystals at 200 ns gate width. Irradiation experiments: radiation 24 h at the 3500 rad/h dose rate

Samples	Light output (p. e./MeV)	Size (mm^3)	Notes
Pure PWO	24.7[a] (51%[b])	$23 \times 23 \times 20$	This paper
PWO:(Sb,Y)	54.2[a] (32%[b])	$23 \times 23 \times 20$	This paper
PWO:Mo	49	$10 \times 10 \times 20$	Ref [5]
PWO:Gd	33	$10 \times 10 \times 25.5$	Ref [5]
PWO:Sb	41	$10 \times 10 \times 20$	Ref [14]
PWO:Y	40	$10 \times 10 \times 20.5$	Ref [7]

[a] LY_0 (light output before irradiation).
[b] Light output loss $= (LY_0 - LY_{irra})/LY_0 \times 100\,\%$; LY_{irra}: light output after irradiation.

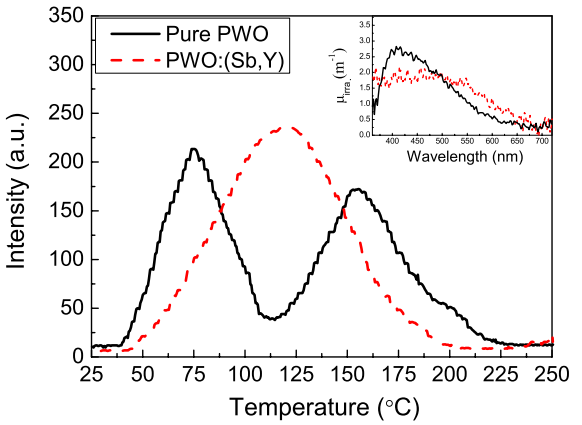

Fig. 6. TL glow curves of pure PWO and PWO:(Sb,Y) single crystals between RT and 250 °C after UV irradiation for 20 min. In the inset, the irradiation induced absorption coefficient ($\mu_{irra.}$) of pure PWO and PWO:(Sb,Y) crystals at the radiation dose: 3500 rad/h for 24 h.

Due to PbO evaporation in the process of PWO growth, a large amount of lead vacancies (V_{Pb}) existed in as-grown PWO, and led to the formation of 350–430 nm absorption band in pure PWO [15]. The 350–430 nm absorption band was tentatively attributed to the formation of mobile color centers (Pb^{3+} and O^-) [12,16] or defect clusters ($[O_2^{3-}–V_{Pb}–V_O–V_{Pb}–O_2^{3-}]$ and $[O_2^{3-}–V_{Pb}–O_2^{3-}]$) [17]. The charge equilibrium modes of doped rare-earth ions (Re^{3+}) were proved by the observation of dielectric relaxation in PWO:La^{3+} crystal [18]. The observed polarization was attributed to the formation of stable $[2(La_{Pb}^{3+})–V''_{Pb}]$ dipole complexes. In addition, the computational simulation results [19] also showed that trivalent ions introduced positive charge defect (Re_{Pb}^{3+}) was compensated by V_{Pb} in the form of $[2(Re_{Pb}^{3+})–V''Pb]$. So in the co-doped PWO:(Sb,Y) crystal, the Sb^{3+} and Y^{3+} ions introduced extra positive charge at the Pb^{2+} sub-lattice, and suppressed the hole centers mentioned above by forming stable $[2(Sb_{Pb}^{3+})–V''Pb]$ and $[2(Y_{Pb}^{3+})–V''Pb]$ dipole complexes, resulting in improving the scintillation properties and radiation harness of PWO. However, it can also be seen that no significant improvement in radiation hardness was obtained in PWO:(Sb,Y) (Fig. 6 inset). This complicated result is different from the case of the other ions having a stable single state [13], and may be due to the oscillation of the Sb ion between the two charge states Sb^{3+} and Sb^{5+}. During the growth of PWO:(Sb,Y) crystal at high-temperature conditions, part of Sb^{3+} ions would be oxygenated into Sb^{5+}. Sb^{5+} ion is similar to Li^+ and Zr^{4+}; for the Zr^{4+} ion doping in $PbWO_4$, it has been reported that this ion possibly enters interstitial sites of $PbWO_4$ crystals [14,20]. Compared to Li^+ and Zr^{4+} ions, Sb^{5+} ion has smaller ionic radius (Zr^{4+} 0.84 Å, Li^+ 0.78 Å, Sb^{5+} 0.62 Å). Therefore, it is more reasonable for Sb^{5+} ions to go into occupying mostly the interstitial site. The introduced positive charges at the interstitial Sb^{5+} sites might be compensated by the random distributed Pb vacancies by means of a long distance compensation. This situation may have some effect on the radiation hardness of PWO:(Sb,Y) crystal. The real reason is not yet clear, so further research work is needed.

4. Conclusions

Co-doped PWO:(Sb,Y) has been grown by modified Bridgman method. The XRD rocking curve shows that the as-grown PWO:(Sb,Y) single crystal is of good quality. Optical transmission in the PWO:(Sb,Y) single crystals significantly improved, and its optical absorption edge became sharper. The Sb and Y co-doping can enhance the luminescence of PWO and make some contributions to the "slow" decay components. Sb^{3+} and Y^{3+} ions are tentatively considered to occupy mostly the V_{Pb}. In PWO:(Sb,Y) two TL peaks existing in pure PWO at around 75 and 155 °C are almost eliminated; however, a new large broad TL peak with a higher intensity appears at about 120 °C. The radiation damage of PWO:(Sb,Y) shows almost no significant improvement. It maybe related to the oscillation of the Sb ion between the two charge states Sb^{3+} and Sb^{5+}. For making more clear the nature of the doping mechanism of PWO:(Sb,Y) and the processes of energy transfer and storage in PWO structure, further work is needed.

Acknowledgements

This work is supported by the Science Innovation Foundation of Shanghai Institute of Ceramics, China.

References

[1] F.A. Kroger, Some Aspects of the Luminescence in Solids, Elsevier, Amsterdam, 1948.
[2] CMS Collaboration, The Compact Muon Solenoid-Technical Proposal, CERN/LHCC 94-38, LHCC/P1, December, 1994.
[3] V.G. Baryshevsky, M.V. Korzhik, V.I. Moroz, V.B. Pavlenko, A.S. Lobko, A.A. Fyodorov, V.A. Kachanov, V.L. Solovjanov, B.I. Zadneprovsky, V.A. Nefyodov, P.V. Nefyodov, B.A. DorogovinL, L. Nagornaja, Nucl. Instr. Meth. A 322 (1992) 231.
[4] K. Nitsch, M. Nikl, S. Ganschow, P. Reiche, R. Uecker, J. Crystal Growth 165 (1996) 163.
[5] M. Kobayashi, Y. Usuki, M. Ishii, M. Nikl, Nucl. Instrum. Methods A 486 (2002) 170.
[6] R. Mao, X. Qu, G. Ren, D. Shen, S. Stoll, C. Woody, Z. Yin, L. Zhang, R. Zhu, Nucl. Instr. Meth. A 486 (2002) 196.
[7] M. Kobayashi, Y. Usuki, M. Ishii, N. Senguttuvan, K. Tanji, M. Chiba, K. Hara, H. Takano, M. Nikl, P. Bohacek, et al., Nucl. Instr. Meth. A 434 (1999) 412.
[8] A. Annenkov, A. Borisevitch, A. Hofstaetter, M. Korzhik, V. Ligun, P. Lecoq, O. Missevitch, R. Novotny, J.P. Peigneux, Nucl. Instr. Meth. A 450 (2000) 71.
[9] S. Wang, D. Shen, G. Ren, Z. Yin, et al., Acta Opt. Sinica 20 (8) (2000) 1122 (in Chinese).
[10] X. Qu, L. Zhang, R. Zhu, Q. Deng, J. Liao, Z. Yin, Nucl. Instr. Meth. A 486 (2002) 89.
[11] P. Yang, J. Liao, B. Shen, P. Shao, H. Ni, Z. Yin, J. Crystal Growth 236 (2002) 589.
[12] M. Nikl, K. Nitsch, S. Baccaro, A. Cecilia, M. Montecchi, et al., J. Appl. Phys. 82 (11) (1997) 5758.
[13] B. Liu, C. Shi, Y. Wei, G. Hu, Nucl. Instr. Meth. B 201 (2003) 520.
[14] M. Kobayashi, Y. Usuki, M. Ishii, N. Senguttuvan, K. Tanji, M. Chiba, K. Hara, H. Takano, M. Nikl, P. Bohacek, S. Baccro, A. Cecilia, M. Diemoz, A. Vedda, M. Martini, Nucl. Instr. Meth. A 465 (2001) 428.
[15] A.N. Annekov, et al., Phys. Stat. Sol. (a) 170 (1998) 47.
[16] M. Nikl, K. Nitsch, J. Hybler, J. Chval, et al., Phys. Stat. Sol. (b) 196 (1996) K7.
[17] Q. Ling, X. Feng, Y. Zhang, Phys. Stat. Sol. (a) 181 (2000) R1.
[18] B. Han, X. Feng, J. Appl. Phys. 84 (1998) 2831.
[19] Q. Ling, et al., J. Phys: Condens. Matter 15 (2002) 1963.
[20] W.L. Zhu, H.W. Huang, X.Q. Feng, M. Kobayashi, Y. Usuki, Solid State Commun. 125 (2003) 253.